

# UC Berkeley

## Precision Manufacturing Group

### Title

Modification of surface properties on a nitride based coating films through mirror-quality finish grinding

### Permalink

<https://escholarship.org/uc/item/6dh3x4qr>

### Authors

Katahira, K.  
H. Ohmori  
J. Komotori  
[et al.](#)

### Publication Date

2010-04-20

Peer reviewed



# Modification of surface properties on a nitride based coating films through mirror-quality finish grinding

K. Katahira<sup>a,\*</sup>, H. Ohmori (2)<sup>a</sup>, J. Komotori<sup>b</sup>, D. Dornfeld (1)<sup>c</sup>, H. Kotani<sup>b</sup>, M. Mizutani<sup>a</sup>

<sup>a</sup>RIKEN, Saitama, Japan

<sup>b</sup>Keio University, Kanagawa, Japan

<sup>c</sup>University of California, Berkeley, CA, USA

## ARTICLE INFO

**Keywords:**  
Coating  
Grinding  
Tribology

## ABSTRACT

In this study, we performed a specific precision grinding process in an attempt to improve the mirror-quality finish and tribological characteristics of titanium nitride based coating films (TiN, TiCN, and TiAlN). The ground surfaces were highly smooth with no evidence of cracking, chipping, or peeling, demonstrating that the hard coating films were finished uniformly. For the TiAlN coating, a significant high level mirror-quality finish was achieved with an average roughness  $R_a$  of 4 nm. In addition, for all films, the employed grinding process led to superior tribological characteristics. In the case of the TiN film, the precision grinding process produced a carbon- and copper-rich surface layer, as well as higher compressive residual stress.

© 2010 CIRP.

## 1. Introduction

In order to reduce the cost and energy consumption of machining processes, tools used for cutting, punching, forging, pressing and molding should be improved to have longer life and to require less frequent maintenance [1–4]. The current challenge is to make further improvements to the surface roughness and functionality of hard coating films generated by physical vapor deposition (PVD) and chemical vapor deposition (CVD). For many types of hard coatings, the coating process alone cannot achieve sufficient surface smoothness; a subsequent surface finishing process is required. The necessity to carry out this procedure manually (i.e., hand polishing) represents an inefficiency in the production process and poses the biggest limitation to increasing productivity. In this study, we attempted to improve the mirror-quality finish and tribological characteristics of titanium nitride based coating films (TiN, TiCN, and TiAlN), which are widely used for cutting, punching, forging, pressing and molding tools, by means of a specific precision grinding process. The resulting films were evaluated by a variety of techniques, including detailed surface observations, tribology tests, elemental analysis, and residual stress measurements.

## 2. Experimental procedure

Titanium nitride based coating films (TiN, TiCN, and TiAlN) were generated by arc ion plating, a PVD technique [5]. The deposited films had thicknesses of approximately 8  $\mu\text{m}$ . Speci-

mens of disk-shaped cemented carbide alloy ( $\varnothing 16$  mm, thickness 1.5 mm) were prepared as substrates for coatings.

Fig. 1 shows an image of the compact desktop four-axis grinding machine used in this study. Despite its compactness, it has high machine rigidity and superior positioning resolution (0.1  $\mu\text{m}$  in the X, Y, and Z directions). In addition, the grinding machine has ELID (electrolytic in-process dressing) capability [6–8]; the grinding wheel surface characteristics were constantly maintained at the optimum level, ensuring excellent processing reproducibility. Table 1 shows the conditions used for grinding experiments. Metal(copper)–resinoid hybrid bond grinding wheels (#8000, abrasives of approximately 2  $\mu\text{m}$  in diameter) with diamond abrasives were used for finish grinding. For simplicity, the specimens finished under the above conditions are referred to as the G-series (ground). Table 2 lists the tribology testing conditions. A reciprocating sliding test system was used. The tests were carried out under dry and wet conditions. The surfaces of the specimens were analyzed by scanning electron microscopy (SEM), contact type surface profilometry, X-ray photoelectron spectroscopy (XPS), and X-ray diffraction spectroscopy (XRD).

## 3. Experimental results and discussion

### 3.1. Surface roughness and observation of finished surfaces

Fig. 2 shows the surface roughness of films produced by the coating process and those produced by the additional grinding processes. The grinding process achieves an improved surface finish, with a surface roughness similar to that obtainable by conventional loose abrasive processes such as polishing or buffing. Particularly, in the case of the G(ground)-TiAlN film, the film had a surface roughnesses of approximately  $R_a = 4$  nm and  $R_z = 76$  nm.

\* Corresponding author.

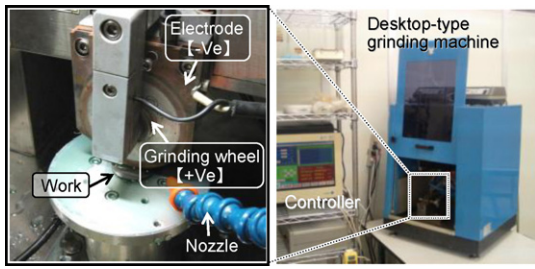


Fig. 1. Overview of desktop-type grinding machine.

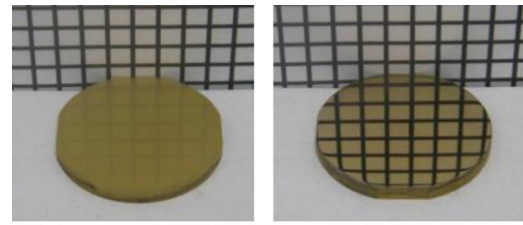


Fig. 3. Macroimages of the as-coated and G-TiN film.

Table 1  
Grinding conditions.

|                       |  |
|-----------------------|--|
| Workpiece             | Titanium nitride based coating films (TiN, TiCN, and TiAlN)                              |
| Grinding machine      | Compact desktop-type 4-axis grinding machine   |
| Grinding wheel        | #8000 metal (copper)–resinoid hybrid bond diamond wheel                                  |
| Grinding fluid        | Chemical solution type grinding fluid (5% dilution to water)                             |
| Grinding conditions   | Wheel rotation: 2000 min <sup>-1</sup> , feed rate: 200 mm/min, depth of cut: 0.2 μm     |
| Electrical conditions | Open voltage: 90 V, peak current: 1 A, pulse timing (on/off): 2/2 μs, pulse wave: square |

Table 2  
Tribology testing conditions.

|                    |   |
|--------------------|---|
| Tribology testing  | Reciprocating sliding test system                     |
| Counter part       | TiN, TiCN, and TiAlN films                            |
| Mating materials   | Al <sub>2</sub> O <sub>3</sub> ball (radius; 4.74 mm) |
| Sliding stroke     | 8 mm  |
| Sliding velocity   | 5 mm/s  |
| Normal load        | 0.98 N  |
| Friction condition | Dry, wet (conventional cutting fluid)                 |

Fig. 3 shows images of the as-coated and G-TiN film, where the mirror-quality finish of the latter can be clearly seen. Fig. 4 shows surface microscopic views of the as-coated and ground series for each type of film. In the as-coated series, numerous scattered droplets are observed; these correspond to unmelted target alloy. After the grinding process, highly smooth and uniform surfaces can be seen. In particular, the droplets of the TiAlN films were removed smoothly, as indicated by the arrow in Fig. 5. Detailed SEM images of the interface between the coating film and the substrate for the G-TiAlN series are shown in Fig. 6. In this case, the specimens were ground with a tapered section method. The surface is highly smooth, and no evidence of cracking, chipping, or peeling is observed, suggesting that the TiAlN film was finished uniformly. These results demonstrate that highly smooth surfaces can be consistently produced by the grinding process using fine abrasives.

Fig. 7 shows cross-sectional views of the G-TiN series samples. The figure clearly shows that the thickness of ground films is varied by changing the total depth of cut. This result indicates that film thickness can be precisely controlled by adjusting the total depth of cut.

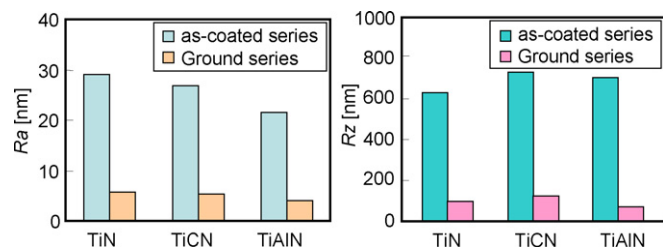


Fig. 2. Surface roughness Ra, Rz.

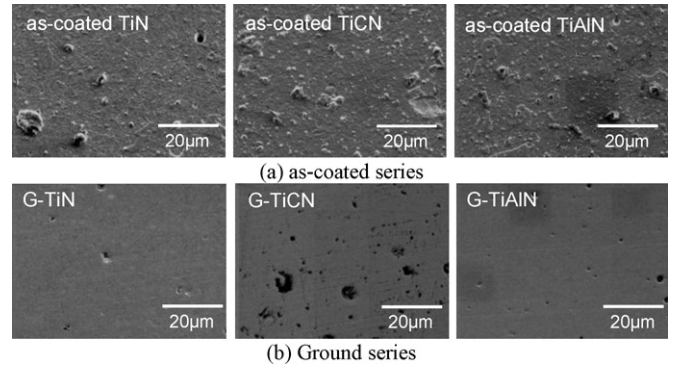


Fig. 4. Surface topographies of the as-coated and ground series for each type of film.

### 3.2. Evaluation of tribological characteristics

#### 3.2.1. Tribological characteristics under dry conditions

Fig. 8(a)–(c) shows the results of sliding friction testing carried out on the TiN, TiCN, and TiAlN films, respectively. In particular, the effects of surface finishing can be clearly seen for the TiN films shown in Fig. 8(a). The friction coefficient of the as-coated TiN film initially increased with sliding cycles up to 250, thereafter maintaining a value of 0.8–1.2. The values were not well constrained, exhibiting a high degree of scatter indicative of unstable behavior. The friction coefficient of the G-TiN film is lower than that of the as-coated TiN film for all numbers of sliding cycles. Although the friction coefficient is dependent on the test conditions, its value for the G-TiN film is approximately one-fourth that of the as-coated TiN film. Fig. 9(a) and (b) shows the wear tracks on the as-coated and ground TiN films. The tracks are about 110 nm deep in both films, but the as-coated TiN film was the only one to show cracks in the film within the wear tracks. These damaged locations seem to be one of the causes of the unstable friction behavior of the as-coated film.

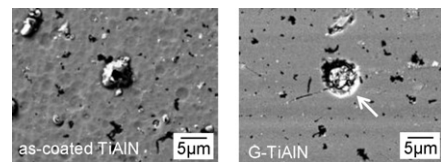


Fig. 5. Droplets of TiAlN films.

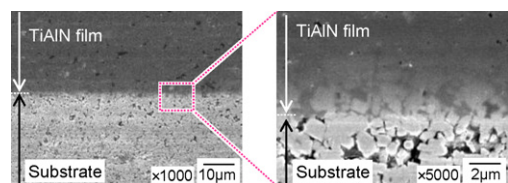


Fig. 6. Detailed SEM images of the interface between the coating film and the substrate for the G-TiAlN series.

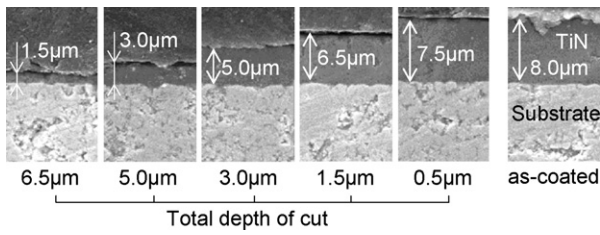


Fig. 7. Cross-sectional views of the G-TiN series.

Fig. 8(b) shows a similar trend for the TiCN films; in comparison with the as-coated TiCN film, the G-TiCN film exhibited a low friction coefficient and very stable tribological behavior.

In the case of the TiAlN films shown in Fig. 8(c), the friction coefficient of the G-TiAlN film was initially low at about 0.4, and gradually increased with sliding distance. However, it remained lower than that of as-coated TiAlN film. The data show very little scatter, indicating very stable tribological behavior.

### 3.2.2. Tribological characteristics of TiN films under wet conditions

Friction tests under wet conditions were also carried out on TiN films, and the results are shown in Fig. 10. A conventional cutting fluid was supplied to the point of contact between the films and an Al<sub>2</sub>O<sub>3</sub> ball such as that shown in the inset. The G-TiN and as-coated films both show stable behavior, and the results indicate that the friction coefficient  $\mu$  of the G-TiN film is lower than that of as-coated film even under wet conditions. Fig. 11 shows the wear tracks for both films after the friction tests. The wear track of the G-TiN film is considerably narrower than that of the as-coated TiN film. Fig. 12 shows the results of SEM observations of the Al<sub>2</sub>O<sub>3</sub> balls after the friction tests. In the case of the G-TiN film, a smooth surface is seen between the wear tracks on the ball, whereas severe

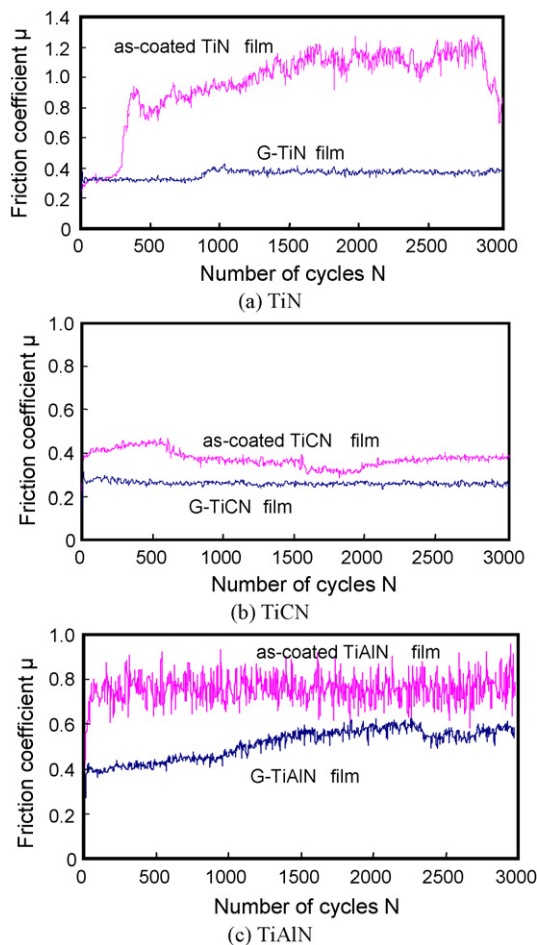


Fig. 8. Results of sliding friction testing.

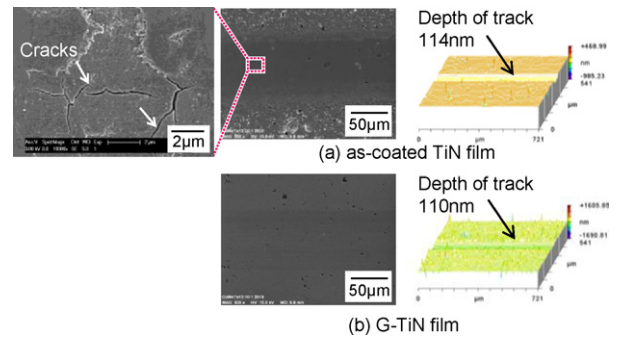


Fig. 9. Wear tracks on the as-coated and ground TiN films.

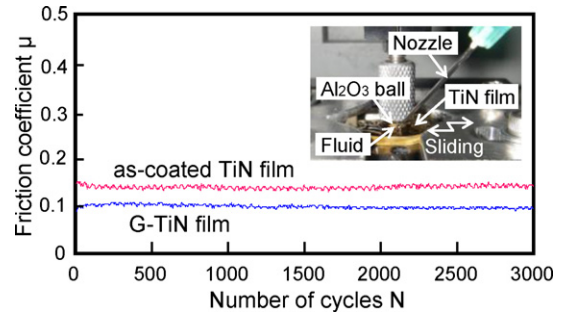


Fig. 10. Results of friction tests under wet conditions.

wear resembling intergranular fracture is observed for the case of the as-coated film. Although both had stable friction coefficients, the film surfaces had widely different appearances following wear and widely different levels of aggressivity toward the contacting material (Al<sub>2</sub>O<sub>3</sub>). We speculate that one of the reasons why the G-TiN film shows such lower friction coefficient under wet conditions is that the many dimples formed when the droplets were removed during grinding had the same effect as fluid reservoirs [9].

### 3.3. Analysis of surfaces of coating film

#### 3.3.1. Chemical analysis of surfaces of TiN films

The properties of the ground TiN surface were investigated by chemical element analysis using XPS. Fig. 13(a) and (b) shows spectral peaks in the vicinity of the carbon binding energy (285 eV) and the copper binding energy (933 eV), respectively. The etching depth is approximately 10 nm in both cases. As shown in the figure, the peaks for the two elements are sharper in the G-TiN film than in the as-coated film. Fig. 14 shows a copper elemental analysis profile in the depth direction. This figure clearly confirms the diffusion of elemental copper from the surface to a depth of about 30 nm. These results suggest that during the grinding process the abrasives (C) and bonding material (Cu) penetrated and diffused into the workpiece surfaces by tribochemical reaction at the grinding contact points. Although this section describes only the diffusion of elemental carbon and copper in the TiN films, diffusion of elemental O and N, which are lighter elements, has been recognized even in TiAlN films [8]. These results raise the

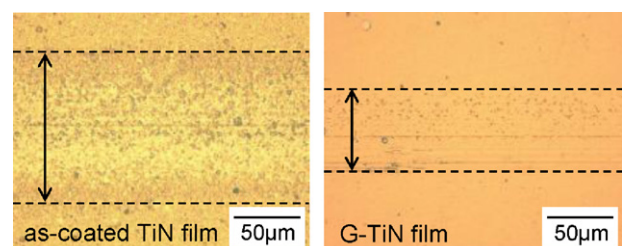


Fig. 11. Wear tracks for both films after the friction tests.



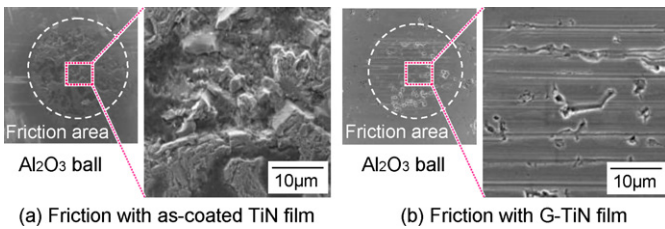


Fig. 12. Results of SEM observations of the  $\text{Al}_2\text{O}_3$  balls after the friction tests.

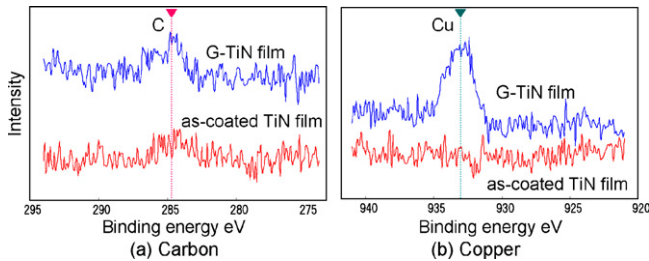


Fig. 13. Spectral peaks in the vicinity of the carbon and the copper binding energy in the case of TiN films.

possibility of controlling diffusion of elements into processed surfaces by selecting processing conditions.

### 3.3.2. X-ray residual stress measurements

Generally, hard coating films contain high residual stresses, and these are known to have a large influence on the functionality of the film. In this section, the residual stresses in a TiN film were measured before and after grinding, in order to examine the effect of grinding on the stress. Measuring residual stresses is generally difficult, but for this analysis, in addition to the conventional  $\sin^2 \psi$  method, the Constant Incidence Angle (CIA) method was used for a more precise determination of stress [10]. In this method, the depth of penetration of an X-ray beam is kept constant to perform extremely precise measurement of the residual stress in the surface layer region. The overall stress in the film was evaluated using the  $\sin^2 \psi$  method, and the CIA method measured the stress to a depth of about  $0.8 \mu\text{m}$  from the surface. Fig. 15 shows the results measured by the two methods. When the residual stresses before and after grinding are compared, both the  $\sin^2 \psi$  method and the CIA method showed high stress values. The  $\sin^2 \psi$  method indicates slightly higher stresses than the CIA method. The mechanism that increases the compressive residual stresses in the hard coating film during grinding is not yet clear, but this is an extremely interesting result. One possible cause of this increase is the influence of the elemental diffusion into the surface layer described in Section 3.3.1. Also, since compressive residual stresses act to suppress the generation of cracks, the absence of cracking in the G-TiN film in Fig. 9 may also be due to this effect. Further experiments are planned in order to clarify the details of the generation mechanism of the compressive residual stress.

## 4. Conclusions

In this study, we performed a specific precision grinding process in an attempt to improve the mirror-quality finish and tribological characteristics of titanium nitride based coating films (TiN, TiCN, and TiAlN), which are widely used for cutting, punching, forging, pressing and molding tools. The ground surfaces were highly smooth with no evidence of cracking, chipping, or peeling,

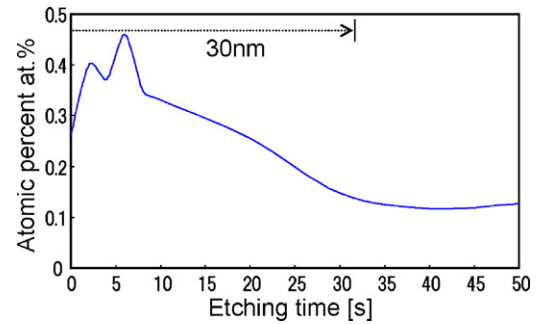


Fig. 14. Copper elemental analysis profile in the depth direction.

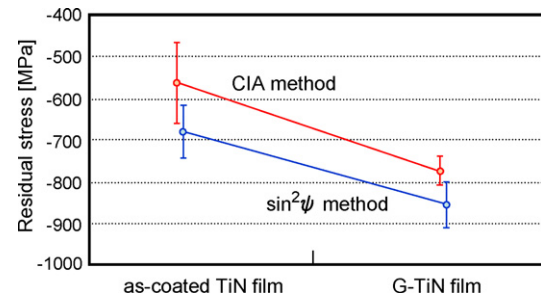


Fig. 15. Residual stresses measured by the two methods.

demonstrating that the hard coating films were finished uniformly. For the TiAlN coating, a significant high level mirror-quality finish was achieved with an average roughness  $R_a$  of 4 nm. In addition, for all films, the employed grinding process led to superior tribological characteristics. In the case of the TiN film, the precision grinding process produced a carbon- and copper-rich surface layer, as well as higher compressive residual stress. The results of this study suggest that the performed precision grinding is highly effective for improving surface qualities and tribological characteristics of practical tools, dies and molds.

## References

- [1] Westkamper E (2008) Manufacture and Sustainable Manufacturing. *Proceedings of the 41st CIRP Conference "Manufacturing Systems"*, Tokyo, 11–14.
- [2] Kopac J (2009) Achievements of Sustainable Manufacturing by Machining. *Journal of Achievements in Materials and Manufacturing Engineering* 34/2:180–187.
- [3] Dornfeld D, Wright P (2007) Technology Wedges' for Implementing Green Manufacturing. *Transactions of the North American Manufacturing Research Institute of SME* 35:193–200.
- [4] Dornfeld D, Min S, Takeuchi Y (2006) Recent Advances in Mechanical Micro-engineering. *Annals of the CIRP* 55/2:745–768.
- [5] Oh SM, Rhee BG, Jeong BS (2003) Wear Behaviors of Ceramics TiN, TiC and TiCN with Arc Ion Plating. *Journal of Mechanical Science and Technology* 17/12:1904–1911.
- [6] Ohmori H, Nakagawa T (1995) Analysis of Mirror Surface Generation of Hard and Brittle Materials by ELID Grinding with Superfine Grain Metallic Bond Wheels. *Annals of the CIRP* 44/1:287–290.
- [7] Ohmori H, Katahira K, Mizutani M, Komotori J (2005) Investigation of Substrate Finishing Conditions to Improve Adhesive Strength of DLC Films. *Annals of the CIRP* 54/1:511–514.
- [8] Katahira K, Watanabe Y, Ohmori H, Kato T (2002) ELID Grinding and Tribological Characteristics of TiAlN Film. *International Journal of Machine Tools & Manufacture* 42:1307–1313.
- [9] Wakuda M, Yamauchi Y, Kanzaki S, Yasuda Y (2003) Effect of Surface Texturing on Friction Reduction between Ceramic and Steel Materials under Lubricated Sliding Contact. *Wear* 254/3–4:356–363.
- [10] Yanase E, Nishio K, Kusumi Y, Arai K, Akiniwa Y, Tanaka K (2002) A Constant Incidence Angle Method to Estimate the Subsurface Distribution of Residual Stress by High-Energy X-Rays from Synchrotron Radiation Source. *Journal of Society of Material Sciences* 51/12:1429–1435.